Nematic LC modes and LC phase gratings for reflective spatial light modulators

by K. H. Yang
M. Lu

Single-domain nematic liquid crystal (LC) devices based on the polarization-rotation effect, the birefringent effect, or both have been investigated for reflective spatial light modulators (SLMs) which use a polarizing beam splitter to separate the input light beam from its orthogonal output beam. We have evaluated each LC mode in terms of its contrast ratio, optical efficiency, operating voltage, and tolerance to cell-gap nonuniformity. We studied the hybrid-aligned and the 0°-, 45°-, and 63.6°-twisted nematic LC modes, which can be operated either normally white (NW) or normally black (NB). We have also investigated the mixed twisted nematic (MTN) and self-compensated twisted nematic (SCTN) modes in NW and the tilted homeotropic mode in NB. Two-dimensional simulations have also been carried out for both NW and NB modes implemented in active-matrix-driven reflective SLMs to elucidate the effect of fringe fields, which tend to generate disclination lines in high-field on-pixels adjacent to low-field off-pixels. Numerical examples are given to illustrate that, for the NB modes, the disclination lines occurring in the field-on bright state appear dark and reduce the optical efficiency. However, for the NW modes, the disclination lines occurring in the field-on dark states generate a light leakage which degrades the contrast ratio. To improve optical efficiency, we have also studied polarization-independent LC phase gratings using patterned alignment with opposite twist angles for reflective SLMs. The basic equations for the diffracted and nondiffracted intensities have been derived. The device parameters, operating voltage, and optical efficiency are given for various cases with a twist angle equal to or less than 90°.

Introduction

It is well known that reflective spatial light modulators (SLMs) offer some advantages over transmissive SLMs, such as increased aperture ratio and more compact optical systems [1]. Recently, Alt [1] and Melcher et al. [2] reported a prototype rear projector having a resolution of 2048 by 2048 pixels using three Si-wafer-based liquid

0018-8646/98/$5.00 © 1998 IBM

crystal (LC) SLMs which utilized a 45°-twisted nematic [or hybrid field-effect (HFE)] mode [3].

Liquid crystals have been widely employed as the display medium for both transmissive and reflective SLMs. In general, the electric-field-tuned LC medium can modulate incident light by one of the following effects: birefringence, polarization rotation, absorption, or scattering. For the active-matrix (AM)-driven transmissive SLMs, the polarization-rotation effect of a 90°-twisted nematic (TN) cell has most frequently been utilized. Operated in the normally white condition, the TN cell for a transmissive display has the advantages of a single cell gap for red, green, and blue colors, low operating voltage, high contrast ratio, high optical efficiency, and insensitivity to variation in cell gap. However, for reflective SLMs with a reflective electrode built inside the LC cell, the TN cell is not useful, because there is no place for a second crossed polarizer. Among reflective nematic LC modes, there is no direct analogy to the transmissive TN mode. Therefore, finding the best LC mode for reflective SLMs is very important.

In this paper, we evaluate single-domain nematic liquid crystal (LC) devices based on the polarization-rotation effect, the birefringence effect, or both for reflective SLMs which use a polarizing beam splitter to separate the input light beam from its orthogonal output beam. We study each LC mode in terms of its contrast ratio, optical efficiency, operating voltage, and tolerance to cell-gap nonuniformity. Our studies include the hybrid-aligned and the 0°-, 45°-, and 63.6°-twisted nematic LC modes, which can all be operated in either the normally white (NW) or normally black (NB) modes. We have also investigated the mixed twisted nematic (MTN) and self-compensated twisted nematic (SCTN) modes for NW and the tilted homeotropic mode for NB. In general, the NW modes have better tolerance to cell-gap nonuniformity than the NB modes, except for the tilted homeotropic mode. We have evaluated the display performance of each LC mode in detail.

Since the pixel for reflective SLMs is usually very small, the effect of fringe fields between high-field on-pixels and low-field off-pixels becomes important. In order to study the fringe-field effect, we have carried out two-dimensional simulations to study LC director[1] orientations and light reflectance as a function of position for reflective active-matrix-driven SLMs. Numerical examples are given for both the NB and NW modes to illustrate the importance of fringe-field effects.

Since the polarization-dependent LC devices use only half of the incident light, it is worthwhile to study the scattering or diffracting LC devices which are polarization-independent and hence offer the potential for a factor-of-2 increase in optical efficiency. The last part of this paper is devoted to the study of polarization-independent LC phase gratings made by patterned alignment with opposite twist angles for reflective SLMs. We derive the general equations for diffracted and nondiffracted intensities using a Jones-matrix approach. We study the operating voltage and the optical diffraction efficiency for various pattern-aligned LC phase gratings with twist angles equal to or less than 90°. The results for several LC phase gratings have been tabulated and compared.

Single-domain nematic LC modes

Using nematic LC mixtures with positive dielectric anisotropy,[2] the construction of single-domain nematic LC cells is relatively simple. The nematic LC medium has a thickness, d, and is sandwiched between two substrates, with the top substrate being transparent and the bottom substrate having a reflective electrode adjacent to the LC medium. There usually exist LC alignment layers such as rubbed polyimide films between the substrates and the LC medium to align the LC director parallel to the rubbing direction with a small pretilt angle (~1°–5°) from the substrate plane. The LC director twists through the LC medium from the bottom toward the top substrate with a total twist angle, Φ. The Jones matrix [4] of such a reflective nematic LC cell can be written[3] [5] as

$$J(\Phi, \beta) = \begin{pmatrix} (\Phi/\gamma)^2 + (\beta/\gamma)^2 \cos 2\gamma - i(\beta/\gamma)\sin 2\gamma & -i\Phi\beta(1-\cos 2\gamma)/\gamma^2 \\ -i\Phi\beta(1-\cos 2\gamma)/\gamma^2 & (\Phi/\gamma)^2 + (\beta/\gamma)^2 \cos 2\gamma + i(\beta/\gamma)\sin 2\gamma \end{pmatrix}, \quad (1)$$

where $\beta = \pi d\Delta n/\lambda$, $\gamma = \sqrt{\beta^2 + \Phi^2}$, and $\Delta n = n_e - n_o$ are the difference between the indices of refraction of the extraordinary and ordinary rays of the LC medium, and λ is the wavelength of the incident light.

Since we are interested in this paper only in LC SLMs which use a polarizing beam splitter to separate the incident beam from the orthogonal output beam, there are three important parameters, Φ, β, Ψ, where Ψ is the angle between the polarization direction of the incident light and the LC director adjacent to the entrance side of the glass plate. By changing these three parameters, we can completely describe the following LC modes: 0°-, 45°-,

[1] The term *director* refers to the direction of the long molecular axis of liquid crystal.

[2] In positive dielectric anisotropy, the difference between dielectric constants along and perpendicular to the LC director is positive.

[3] Our results are different in sign from the results of Lu and Saleh [5].

63.3°-twisted, mixed TN, and self-compensated TN. Once we choose an LC mode, the values for Φ and Ψ are fixed. The only common variable parameter for all of these modes is β.

Assuming that the polarized incident light is a P-wave, the reflected signal will be an S-wave orthogonal to the P-wave. We can calculate the P-to-S conversion efficiency (PCE) of various LC modes as a function of $d\Delta n/\lambda$. By our definition, the PCE characterizes the effect due to the LC medium alone, neglecting loss due to reflection from all surfaces. The results are shown in **Figure 1** for the 0°-, 45°-, and 63.6°-twisted modes and in **Figure 2** for the mixed TN (MTN) and self-compensated TN (SCTN) modes. The values of Φ and Ψ for different LC modes associated with Figures 1 and 2 are explained below.

Homogeneous (or 0°-twisted) LC mode

In this mode, $\Phi = 0°$ and $\Psi = 45°$; the LC cell behaves as a birefringent plate with its optical axis at 45° with respect to the crossed polarizer and analyzer. In the literature [6] it is also referred to as parallel-aligned mode. The equation to calculate the PCE can be written as

$$I_{PS} = \sin^2(2\pi d\Delta n/\lambda), \tag{2}$$

and its results as a function of $d\Delta n/\lambda$ are shown in Figure 1 as the solid curve. We can operate this mode as NW or as NB. For the NB case, I_{PS} should be as small as possible when the applied voltage is below the threshold voltage. To satisfy the above condition, there are multiple choices for the cell gap satisfying the equation $d\Delta n/\lambda = 0.5, 1, 1.5, 2, \cdots$ corresponding to half-wave plate, full-wave plate, etc. The voltage required to drive these modes with maximum PCE is quite low (less than 3.5 V) for the case of the half-wave plate and progressively lower for the case of the full-wave plate, etc. One always chooses the half-wave plate to achieve faster response for the SLM. However, it requires stringent cell-gap uniformity to achieve a high contrast ratio. From Equation (2), it can easily be derived that, for contrast ratios larger than 100 to 1, $|\Delta d/d|$ must be less than 0.032. Equivalently, for a broadband incident light with $\Delta\lambda/\lambda > 0.032$, it is impossible to obtain contrast ratios that are larger than 100 to 1. Hence, this mode is only suitable for nearly monochromatic incident light with stringent requirements on cell-gap uniformity.

We can also operate the homogeneous LC mode as NW. Again, there are multiple choices for the cell gap satisfying the condition $d\Delta n/\lambda = 0.5n + 0.25$, where n is an integer. One usually takes $n = 0$ to satisfy the quarter-wave condition. In this quarter-wave NW mode, the PCE decreases as the applied voltage increases across the LC cell. However, it requires a relatively high voltage (usually larger than 15 V) to achieve a sufficiently dark state for a

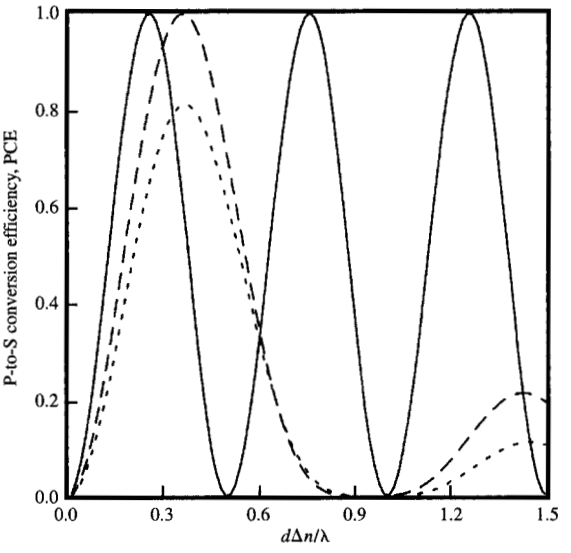

Figure 1

Polarization conversion efficiency (PCE) as a function of $d\Delta n/\lambda$. The solid, dot, and dash curves are for 0°-, 45°-, and 63.6°-twisted LC modes, respectively.

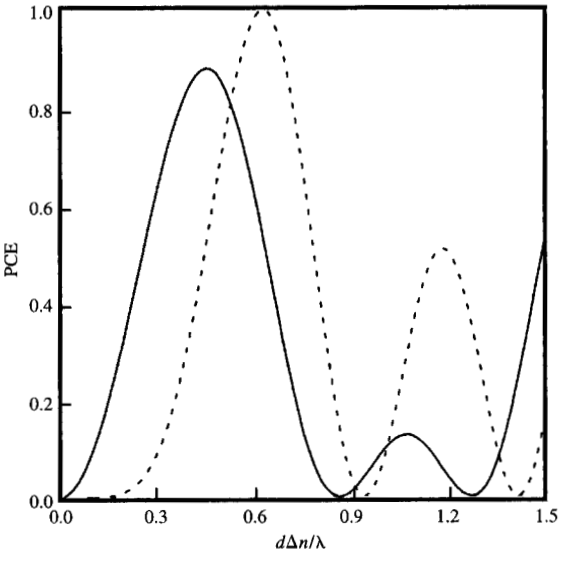

Figure 2

PCE as a function of $d\Delta n/\lambda$. The solid and dot curves are for mixed TN and self-compensated TN, respectively.

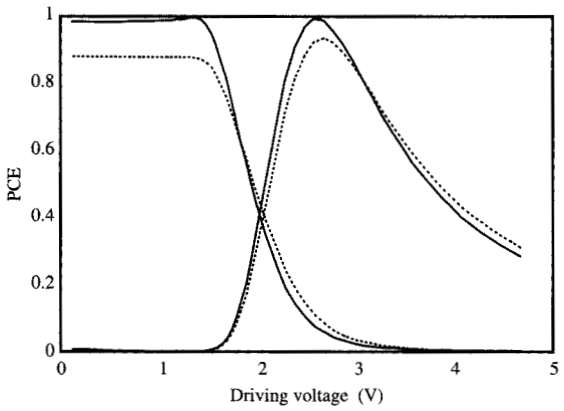

Figure 3

Calculated PCE as a function of applied voltage using data for LC mixture MLC13200-100 from Merck and the parameters listed in Table 1. The solid curves are for NW SCTN and NB 54°-twisted modes, while the dashed curves are for NW MTN and NB 45°-twisted modes.

Table 1 Parameters used for the calculation of Figure 3 with incident wavelength at 546 nm.

Device	*Mode*	$\Delta nd/\lambda$
MTN	NW	0.45
SCTN	NW	0.62
45°-twist	NB	0.97
54°-twist	NB	0.95

high contrast ratio because of the residual birefringent effect caused by the boundary LC layers. The advantage of this mode is the fast response [6], which is sufficient for field sequential color because of its thin cell gap and high operating voltage. The operating voltage can be reduced by placing a properly designed optical compensation film in front of the LC cell. However, the time required to turn on the LC cell increases with a reduced operating voltage.

45°-twisted mode

This mode [3] has $\Phi = 45°$ and $\Psi = 0$ or 90° and has been referred to as the HFE (hybrid field-effect) mode. The equation for the PCE in the case of zero field can be written as

$$I_{PS} = [1 - \pi^2/(16\gamma^2)] \times \pi^2 \sin^4 \gamma/(4\gamma^2), \quad (3)$$

and the results as a function of $d\Delta n/\lambda$ are shown as the dotted curve in Figure 1. For the NB operation, we usually choose $d\Delta n/\lambda = \sqrt{15/16}$ so that $\sin \gamma = 0$ in Equation (3).

In order to find the PCE as a function of applied voltage, we have to carry out further simulations. For the calculation of the LC director profile across the LC cell under an applied electric field, we have used a tensor formulation [7] of LC continuum theory, allowing full elastic anisotropy, chirality, and disclination [8]. Such a method was also applied for the 2D simulation described in a later section of this paper. The extended Jones-matrix method [9] was used to calculate the PCE of LC cells with monochromatic incident light.

The operation voltage for this mode [3] is usually less than 3.5 V. We have verified this low operating voltage by calculating the PCE as a function of applied voltage. The results are shown in **Figure 3**. For the calculation of Figure 3, we used the data for LC mixture MLC13200-100 from Merck & Co., Inc., and other parameters listed in **Table 1**. The cell-gap tolerance for this mode can be derived from Equation (3) and is large, so that, for $|\Delta d/d| \leq 0.11$, the contrast ratio exceeds 200 to 1. The disadvantage of this mode is a low PCE (less than 0.93), as shown in Figure 3. The PCE can be improved to better than 0.99 by changing the twist angle from 45° to about 54° [10]. However, at a twist angle of 54°, the tolerance to cell-gap nonuniformity is slightly less [10] than with the 45°-twisted mode.

We can also operate the 45°-twisted mode as NW by choosing $d\Delta n/\lambda = 0.362$. The advantage is a relatively fast response time because of a thin cell gap as compared to the NB mode, but it requires relatively high voltage to achieve high contrast ratio and has a low PCE (about 0.81).

- *63.6°-twisted mode*

This mode [11] has $\Phi = \pi \div 2\sqrt{2}$ and $\Psi = 0°$ or 90°. The equation for the PCE can be simplified as

$$I_{PS} = \Phi^2\beta^2(1 - \cos 2\gamma)^2/(\gamma^4), \quad (4)$$

and the results as a function of $d\Delta n/\lambda$ are shown in Figure 1 as the dashed curve. We can choose $d\Delta n/\lambda = 0.935$ or 0.354 for NB or NW operation, respectively. The characteristics of 63.6°-twisted NB and NW modes are similar to the corresponding 45°-twisted NB and NW modes, except that the 63.6° NW mode has a nearly 100% PCE, as indicated in Figure 1.

- *Hybrid-aligned cell*

The hybrid-aligned mode [12] is similar to the 0°-twisted mode, except that the LC directors adjacent to one of the cell substrates are aligned perpendicular or nearly perpendicular to the cell substrate. The equation for the PCE can be expressed as in Equation (2) with Δn replaced by $0.5\Delta n$ because the effective birefringence of the hybrid-aligned LC cell is a factor of 2 less than the 0°-twisted

cell. For the NW hybrid-aligned mode, there is no threshold voltage, and it requires a relatively high operating voltage to achieve good dark states because of the existence of residual birefringence due to the boundary LC layers. It has the advantage of fast response time because of a relatively thin cell gap and hybrid alignment, so that an external field exerts a high torque instantaneously on the LC directors in the cell. For the NB operation, it requires very stringent cell-gap uniformity, as in the case of the NB 0°-twisted mode.

- *Mixed TN mode*

The mixed [13] TN mode has $\Phi = 90°$ and $\Psi = 20°$. The PCE of the MTN mode as a function of $d\Delta n/\lambda$ is shown as the solid curve in Figure 2. For the NW operation, the cell gap is chosen to satisfy the equation $d\Delta n/\lambda = 0.45$. We have calculated the PCE as a function of applied voltage, and the results shown in Figure 3 indicate that a voltage larger than 4.5 V is needed for NW MTN. The peak PCE is only 0.88, as shown in Figure 3. However, its turn-on and turn-off times are about four times faster than those of the corresponding 90°-twisted TN cell because of the shorter cell gap. The PCE can be increased by reducing Φ and changing Ψ. However, when this is done, the operating voltage increases. The NW MTN mode has a large tolerance for cell-gap nonuniformity. As far as $|\Delta d/d| < 0.15$, high contrast ratio can be maintained if the dark state is taken at a voltage larger than 4.5 V for most of the useful LC mixtures for AM LCDs. The NB MTN mode is not attractive because it has poor tolerance to cell-gap nonuniformity.

- *Self-compensated TN mode*

The self-compensated [14] TN mode has $\Phi = 60$ to 65° and $\Psi = 0.5\Phi$. The PCE as a function of $d\Delta n/\lambda$ is shown in Figure 2 as the dashed curve for the case $\Phi = 60°$. For the NW operation, we chose the cell gap to satisfy the relation $d\Delta n/\lambda = 0.61$. The PCE can be 100%, and its operating voltage is the lowest among all of the NW modes discussed in this paper. One of the solid curves in Figure 3 shows the calculated results of PCE as a function of applied voltage for the SCTN with a twist angle of 60°, indicating a high PCE and low operating voltage. The low operating voltage is the result of a partial self-compensation [14] effect between two boundary LC layers adjacent to cell boundaries under the external field because the polarization of the incident beam bisects these two boundary LC layers. The NW SCTN mode has a medium tolerance in cell-gap nonuniformity such that $|\Delta d/d|$ should be below about 0.1, and an operating voltage below about 3 V is possible by using an LC mixture with larger dielectric anisotropy, such as TL222 from Merck. The SCTN mode is unsuitable for the NB operation because it requires a stringent cell-gap uniformity.

- *Tilted homeotropic mode*

The tilted homeotropic (TH) mode [15], which is also referred to as the DAP (deformation of aligned phase) or ECB (electric-field-controlled birefringence) mode, is suitable only for the NB operation. For the TH mode, we use nematic LC mixtures with negative dielectric anisotropy, and the LC directors are aligned approximately perpendicular to the substrates of the LC cell, with a small pretilt angle away from the normal of the cell substrate. The TH cell is placed between crossed polarizers whose polarization directions are bisected by the projection of the LC directors onto the cell substrate. When the applied voltage across the TH cell is larger than the threshold voltage, the LC directors within the TH cell are deformed toward the substrate plane, resulting in an equivalent birefringence plate. The PCE of a TH cell under applied external voltage can reach 100% and can be described by the integration of Equation (2) across the cell thickness, where Δn is no longer a constant but depends on the position across the TH cell. The quiescent state is the dark state of the display. The dark state becomes less dark as the pretilt angle from cell normal increases. For high contrast ratio, the pretilt angle from cell normal should be less than ~4° if we choose $d\Delta n/\lambda < 0.5$. The major advantages of the TH cell are extremely high contrast ratio, high PCE, a single LC thickness for red, green, and blue colors, and a very large tolerance to LC thickness nonuniformity (the tolerance is $|\Delta d/d| \geq 0.15$). The disadvantages are difficulty in achieving stable alignment and limited availability of LC mixtures with negative dielectric anisotropy.

Fringe-field effects

The pixel for reflective SLMs is rather small, about 5 to 20 μm. In order to achieve a high aperture ratio, the gap between each pixel electrode is very small, of the order of 1 μm, depending on the photolithographic rules. If a pixel is switched on with the adjacent pixels off, the fringe field between the on-pixel and adjacent off-pixels will generate two effects. Parts of the off-pixel adjacent to the on-pixel will be partially switched on, and parts of the on-pixel will be on to a smaller extent. This will result in a change of the modulation transfer function of the display. The second effect is that disclination lines will be generated within the on-pixel as a result of competition between the normal-tilt domain under uniform field and the reverse-tilt domain generated by the fringe field. In the NB case, the disclination lines appear dark within the bright on-pixel to reduce the effective aperture ratio. However, in the NW case, the disclination lines appear bright within the dark voltage-on pixel, thereby reducing its contrast ratio.

We have carried out a two-dimensional simulation to study the effects of the fringe field on the display. **Figure 4** shows the construction of a 45°-twisted LC mode in a

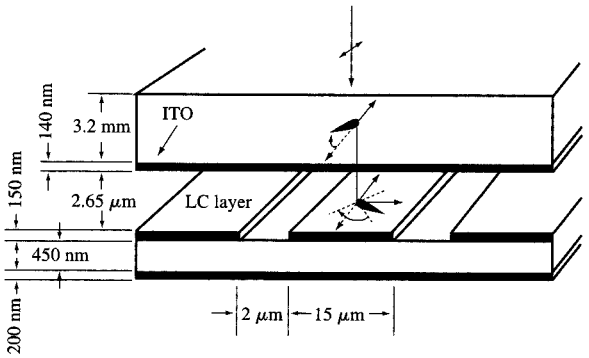

Figure 4

Front view of three pixels (picture elements) illustrated schematically. A two-dimensional 45°-twisted cell used to calculate the LC director orientations and reflectance is sketched on the central pixel.

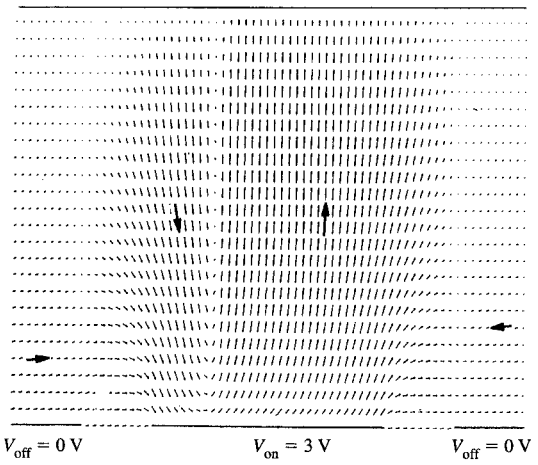

Figure 5

Cross-sectional view of two-dimensional LC director orientations across an on-pixel between two off-pixels. The bars, which correspond to the LC director orientations, point out of the paper toward the reader in the direction of the arrowhead. Grid points are finer in the gap region between pixel electrodes.

reflective SLM. On top of a silicon substrate, we deposited a 200-nm metallic light-absorbing black matrix with $n = 0.89$ and $k = 1.51$, where n and k are the real and imaginary parts of the index of refraction, respectively. A silicon nitride layer of 450 nm was deposited between the black matrix and the Al pixel electrode with a thickness of 150 nm. The pixel is 15 μm, with a gap of 2 μm between the pixel electrodes. The LC cell gap is 2.65 μm and, for the simulation, we used data for the LC mixture TL222 from Merck with a chiral pitch of 32 μm. The indium–tin-oxide (ITO) electrode has a thickness of 140 nm. As shown in Figure 4, the LC directors twist from a position 45° between the x- and $-y$-axes on the pixel electrode to the $-y$-axis on the ITO electrode. The LC directors have a pretilt angle α of 2° from the substrate plane.

To illustrate the fringe-field effect on an NB display, the LC director orientations and reflectance have been calculated along a middle line in the x-axis direction across a three-pixel geometry. Both the ITO electrode and the black matrix are connected to ground potential. In the first case, pixels 1 and 3 are at ground potential, while pixel 2 in the middle is at 3 V. The results for the LC director orientation are shown in **Figure 5**, where the grid points for calculation are finer in the gap region between pixel electrodes. The results indicate that a disclination line located to the left of the center of the on-pixel exists at 3 V. The disclination separates the normal-tilt domain at the right from the reverse-tilt domain at the left. The reverse-tilt domain is caused mainly by the fringe field existing on the left edge of the pixel electrode at 3 V. The calculated reflectance associated with Figure 5 is shown in **Figure 6**, which indicates the existence of a dark disclination line on the bright on-pixel and the fringe field turning a small portion of the adjacent off-pixel partially on. For comparison, we have also calculated the case in which pixels 1 and 3 are at 1.5 V instead of 0 V. The results for the LC director orientation and the reflectance are shown in **Figures 7** and **8**, respectively. Comparing Figures 5 and 7 or Figures 6 and 8, the fringe-field effect is rather insensitive to the off-pixel from 0 to 1.5 V.

To illustrate the effect of fringe field on an NW display, we have also carried out two-dimensional simulation for NW SCTN with a total twist angle of 60° such that the LC directors twist left-handed from the pixel electrode toward the ITO electrode, with the $-y$-axis bisecting the total twist angle. (See Figure 4 for reference.) The data of the LC mixture ZLI3449-100 from Merck were used for simulations. The pixel is 17 μm, with a gap of 1.8 μm between pixel electrodes. The LC cell gap is 2.6 μm. Simulations were made with three pixels using voltages of −2.5, 2.5, and −2.5 V in sequence, with both the ITO electrode and the metallic black matrix grounded. The simulated results for LC director orientations as a function of position along the x-axis are shown in **Figure 9**, and the corresponding reflectance is shown in **Figure 10**. Again, in Figure 9, the grid points are finer around the gap region to elucidate the fringe-field effect. Figure 9 indicates that there exists a reverse-tilt domain around the left edge of the central pixel electrode. There exist two

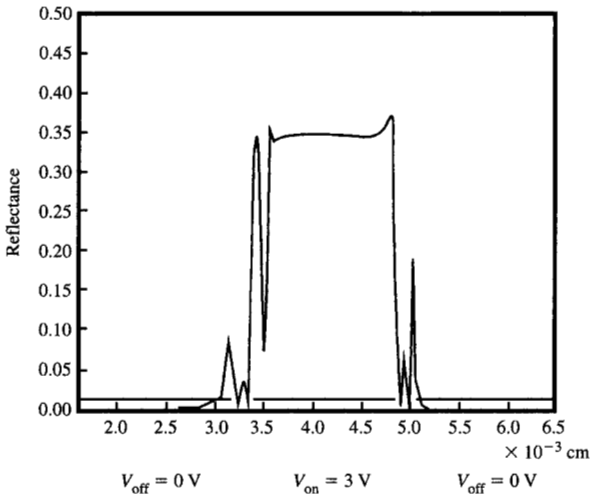

Figure 6

Calculated reflectance as a function of position corresponding to LC director orientations shown in Figure 5.

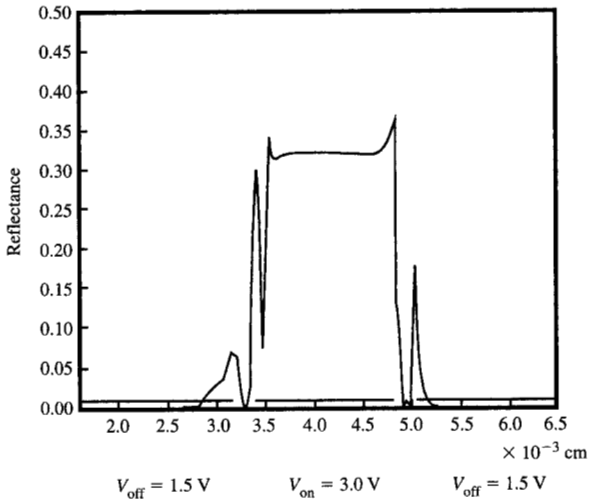

Figure 8

Calculated reflectance as a function of position corresponding to LC director orientations shown in Figure 7.

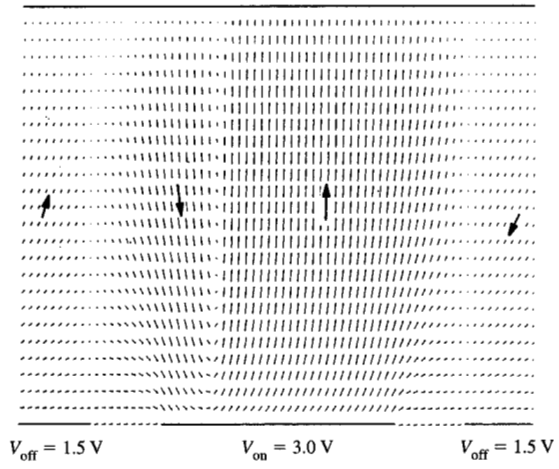

Figure 7

Same as Figure 5 except that the voltage at the off-pixels is 1.5 V instead of 0 V.

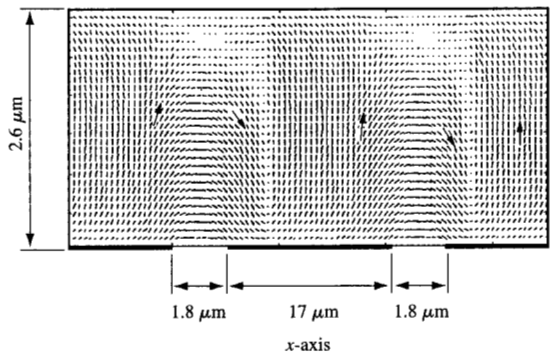

Figure 9

Cross-sectional view of two-dimensional LC director orientations across three pixels with -2.5, 2.5, and -2.5 V, respectively, for a 60°-twisted NW mode. The bars, which correspond to the LC director orientations, point out of the paper toward the reader in the direction of the arrowhead. The grid points are finer around the gap region between pixel electrodes.

disclination lines, one to the left and the other to the right of this reverse-tilt domain. A strong light leakage occurs around each disclination line, as shown in Figure 10. In this case, the light leakage is quite large, so that extreme care must be taken in designing and driving various LC modes for NW operation.

Conclusions concerning single-domain nematic LC modes

We have investigated several different LC modes for reflective SLM applications. The selection of the best LC mode depends on specific applications. In general, NW modes may have a high contrast ratio in test cells, but by

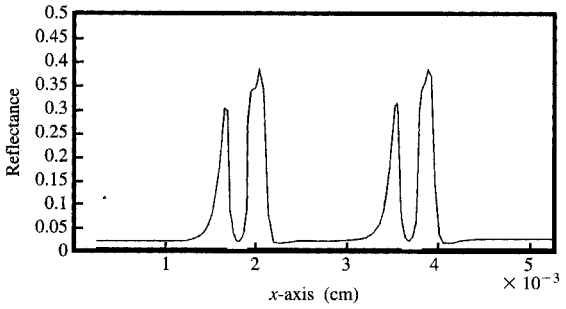

Figure 10

Calculated reflectance as a function of position corresponding to LC director orientations shown in Figure 9.

implementing them on the Si-wafer-based active matrix, a high contrast ratio can be maintained only with a nonreflecting black matrix absorbing the light impinging upon the gaps between pixel electrodes. NB modes are more suitable in the case of a poor black matrix.

For the case of using three SLMs, each for one color, to form a projection display, both NB 54°-twisted and NW SCTN are particularly attractive because of their low driving voltage and high PCE. We have optimized the twist angle of the NB HFE mode to achieve an NB 54°-twisted cell which has nearly 100% PCE, a 7% improvement over the NB HFE (45°-twisted) cell, with a slight reduction in cell-gap tolerance.

Comparing the 54°-twisted NB mode with the TH NB mode, we find that the latter has a slightly larger cell-gap tolerance and higher contrast ratio due to homeotropic alignment, with a relatively low pretilt angle from cell normal. The TH mode is attractive when a high driving voltage (>5 V) is available, and stable uniform alignment with a suitable pretilt angle can be achieved.

For field-sequential color displays using a single cell for full colors, NW modes are generally more favorable than NB modes because of their shorter cell gap, resulting in faster switching speeds. For this application, NW 0°-twisted or 63.6°-twisted mode with an optical compensation film to lower the driving voltage and maintain a high PCE as well as an NW MTN mode with a lower PCE can be used.

Polarization-independent LC phase gratings

It is well known that polarization-dependent reflective or transmissive LC SLMs use only at most half of the incident light intensity without the use of unwanted polarization, which increases *étendue* and cost. Scattering and diffracting LC devices have the potential to utilize all of the intensity of the incident light. LC phase gratings are a polarization-independent alternative to the polarization-dependent LC modes discussed in the first part of this paper. Hori [16] proposed an LC grating design based on field-induced tunable birefringence. However, the untwisted device exhibited polarization-dependent performance and required a high voltage to achieve high contrast. It also required interdigitated electrodes within each pixel, resulting in a possibility of more shorts across electrodes. Fritsch et al. [17] have investigated polarization-independent LC gratings. The result was a reflective device based on the field-controlled birefringence difference between alternating stripes inside each pixel. To avoid using interdigitated electrodes, Shannon et al. [18] suggested the use of pattern alignment to generate phase gratings. Because the differently patterned domains require no separation, diffraction efficiency is increased and the risk of shorts between electrodes is reduced. Bos et al. [19] have demonstrated the use of pattern alignment with an optically active device for transmissive SLMs. High contrast and relatively low-operation voltage have been demonstrated. It is a purpose of this paper to explore the pattern alignment with a periodic unit domain consisting of two equal-size half-domains with opposite twist angle.

In utilizing the polarization-independent LC phase gratings, except for some rare special cases, it is extremely difficult to make the nondiffracted light vanishingly small, so that collecting the nondiffracted light as a signal results in poor contrast. Therefore, in this paper, we consider only the case of collecting the diffracted light as a signal.

Following Equation (1), we can write the output E-field $[E_{xo}, E_{yo}]$ after an interference between two domains with opposite twist angles in terms of the input E-field $[E_{xi}, E_{yi}]$ as

$$\begin{bmatrix} E_{xo} \\ E_{yo} \end{bmatrix} = ([J(\Phi, \beta)] + [J(-\Phi, \beta)]) \begin{bmatrix} E_{xi} \\ E_{yi} \end{bmatrix}. \quad (5)$$

The resulting intensity, which represents nondiffraction intensity, can be written as

$$I_o = |E_{xo}|^2 + |E_{yo}|^2 = [(\Phi/\gamma)^2 + (\beta/\gamma)^2 \cos 2\gamma]^2 + (\beta/\gamma)^2 (\sin 2\gamma)^2. \quad (6)$$

The diffracted intensity due to interference between two domains can be expressed as

$$I_d = [\Phi\beta/(\gamma)^2(1 - \cos 2\gamma)]^2. \quad (7)$$

From Equation (6), we see that in order to have the nondiffracted (or zero-order-diffraction) intensity I_o equal to zero, the following two conditions must be satisfied:

$$(\Phi/\gamma)^2 + (\beta/\gamma)^2 \cos 2\gamma = 0 \quad (8)$$

Table 2 Summary of parameters for LC phase gratings.

Φ	$\beta = \Delta nd/\lambda$	*Mode*	I_D *(max.)* (%)	*Voltage [9]* (V)
0.5π	0.355	NWD	69.4	3.3
0.5π	0.866	NBD	33.0	2.2
0.3536π	0.354	NWD	90.2	>5
0.3536π	0.935	NBD	91.8	2.4
0.3π	0.36	NWD	100	>5
0.3π	0.954	NBD	93.9	2.4
0.25π	0.365	NWD	81.4	>5
0.25π	0.968	NBD	93.5	2.5

and

$$\beta(\sin 2\gamma)/\gamma = 0. \tag{9}$$

The solutions for Equations (8) and (9) are

$$\gamma = \left(\frac{2n+1}{2}\right)\pi \text{ and } \Phi = \beta = \frac{\gamma}{\sqrt{2}}, \qquad \text{where } n = 0, 1, 2, \cdots. \tag{10}$$

Substituting (10) into (7), we have $I_d = 1$, so that all of the incident light becomes diffracted. In this case, we have 100% optical efficiency. The Jones matrix becomes

$$J\left(\pm(2n+1)\frac{\pi}{2\sqrt{2}}, (2n+1)\frac{\pi}{2\sqrt{2}}\right) = \pm i\begin{pmatrix} 0 & -1 \\ -1 & 0 \end{pmatrix}. \tag{11}$$

This means that, in the case of 100% optical efficiency, the polarization of incident light has been rotated exactly 90° or −90° by the SLM. According to Equation (10), there are multiple cases having 100% optical efficiency. But, except for the $n = 0$ case, these cases have a twist angle larger than 180° and a large $d\Delta n$, so that the device will have very long response times. One obvious solution for Equation (10) is that when $n = 0$, $\Phi = \beta = \pi/(2\sqrt{2})$. The device is diffractive when $E = 0$, and diffraction decreases as the field increases. We call this a normally white diffractive (NWD) mode. This NWD mode has 100% optical efficiency, a low twist angle, and a thin cell gap resulting in short response times. The disadvantage of this NWD mode is the high driving voltage required because of the residual birefringence effect caused by the boundary LC layers. The diffraction efficiencies of other opposite-twisted two-domain TN LC phase gratings with a twist angle equal to or less than 90° are less than 100%. For the NWD mode, the device parameters, driving voltage, and optical efficiency for different twist angles are listed in **Table 2**. Although the 90° TN phase grating has a low driving voltage, the optical diffraction efficiency is quite low.

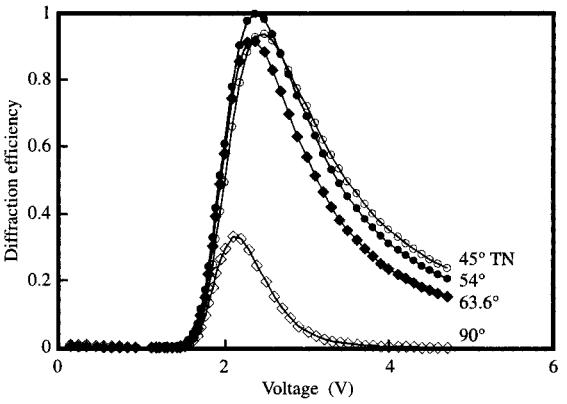

Figure 11

Calculated optical diffraction efficiencies of normally black LC phase ratings as a function of applied voltage using twist angle as a parameter.

In addition to the NWD modes, we can make the device nondiffractive at zero field, becoming diffractive when the field is on. We call these normally black diffractive (NBD) modes. The requirement for the NBD mode is that the off-diagonal terms of the Jones matrix as expressed by Equation (1) be equal to zero in the quiescent state. That is,

$$\Phi\beta/(\gamma)^2(1 - \cos 2\gamma) = 0, \qquad \text{i.e., } \gamma = n\pi. \tag{12}$$

In this case, the Jones matrix becomes a unit matrix at the quiescent state. In Equation (12), once the value of n is chosen, the value of β can be determined for a given Φ. In the on-states, the electric field drives the two reverse-twisted domains into the polarization-rotation state. The driving voltage of the NBD is much lower than the NWD. The optical diffraction efficiencies of the NBD LC phase gratings (calculated for the case of TL222 from Merck) as a function of applied voltage are shown in **Figure 11** for the twist angles of 45°, 54°, 63.6°, and 90°. A diffraction efficiency of nearly 100% can be achieved by using a 54°-twisted instead of 63.6°-twisted LC phase grating because of the nonuniform twist of the liquid crystal molecules in field-on states. For the NBD mode, the device parameters and the estimated optical efficiencies are listed in Table 2.

In conclusion, the NWD LC phase gratings have, in general, high operating voltages, but faster response times than the NBD LC phase gratings. Some of the NBD LC phase gratings have low operating voltages as well as relatively high optical diffraction efficiencies, including

three having twist angles from 45° to 63.6°. The 54°-twisted NBD mode is extremely attractive because of its nearly 100% optical diffraction efficiency and low operating voltage.

Acknowledgment

The authors acknowledge Kun-Wei Lin at Sunplus Technology Co., Ltd., Taiwan, for writing the programs to perform two-dimensional simulations.

References

1. P. M. Alt, "Single-Crystal Silicon for High Resolution Display," *Proceedings of the 1997 International Display Research Conference*, (Society for Information Display), Toronto, September 1997, p. M-19.
2. R. L. Melcher, P. M. Alt, D. B. Dove, T. M. Cipolla, E. G. Colgan, F. E. Doany, K. Enami, K. C. Ho, I. Lovas, C. Narayan, R. S. Olyha, Jr., C. G. Powell, A. E. Rosenbluth, J. L. Sanford, E. S. Schlig, R. N. Singh, T. Tomooka, M. Uda, and K. H. Yang, "Design and Fabrication of a Prototype Projection Data Monitor with High Information Content," *IBM J. Res. Develop.* **42**, No. 3/4, 321–338 (1998, this issue).
3. Jan Grinberg, Alex Jacobson, William Bleha, Leroy Boswell, and Gary Myer, "A New Real-Time Non-Coherent to Coherent Light Image Converter, the Hybrid Field Effect Liquid Crystal Light Valve," *Opt. Eng.* **14**, 217 (June 1975).
4. R. C. Jones, *J. Opt. Soc. Amer.* **32**, 486 (1942).
5. K. Lu and B. E. A. Saleh, "Complex Amplitude Reflectance of the Liquid Crystal Light Valve," *Appl. Opt.* **30**, 2354 (1991).
6. Peter Jansen, Viktor Konovalov, Anatoli Muravski, and Sergei Yakovenko, "Fast Responding Liquid Crystal Light Valve Technology for Color Sequential Display Application," *Proc. SPIE* **2795**, 141 (1996).
7. S. Dickmann, J. Eschler, O. Cossalter, and D. A. Mlynski, "Simulation of LCDs Including Elastic Anisotropy and Inhomogeneous Field," *Digest of Technical Papers*, Society for Information Display International Symposium, 1993, p. 638.
8. K. W. Lin, H. P. D. Shieh, and Feng-Cheng D. Su, "Analysis of Capacitance–Voltage Characteristics for Two-Dimensional Multi-Conductor in Liquid Crystal Displays," *Appl. Phys. Lett.* **68**, 2444 (1996).
9. Claire Gu and Pochi Yeh, "Extended Jones Matrix Method: II," *J. Opt. Soc. Amer. A* **10**, 966 (1993).
10. K. H. Yang and Minhua Lu, "Nematic LC Modes for Liquid-Crystal-on-Silicon Projectors," to be published in *Projection Displays IV*, *Proc. SPIE* **3296** (1998).
11. T. Sonehara and O. Okumura, "A New Twist Nematic ECB (TN-ECB) Mode for a Reflective Light Valve," *Proceedings of Japan Display '89*, 1989, p. 192.
12. J. Glueck, E. Lueder, T. Kallfass, and G. D. Myer, "Color-TV Projection with Fast-Switching Reflective HAN-Mode Light Valves," *Digest of Technical Papers*, Society for Information Display International Symposium, 1992, p. 277.
13. Shin-Tson Wu and Chiung-Sheng Wu, "Mixed-Mode Twisted Nematic Liquid Crystal Cells for Reflective Displays," *Appl. Phys. Lett.* **68**, 1455 (1996).
14. K. H. Yang, "A Self-Compensated Twist Nematic Mode for Reflective Light Valves," *Proceedings of Euro Display '96* (Society for Information Display), 1996, p. 499.
15. Frederic Kahn, "Electric-Field-Induced Orientational Deformation of Nematic Liquid Crystals: Tunable Birefringence," *Appl. Phys. Lett.* **20**, 199 (1972).
16. Y. Hori and K. Asai, "Field Controllable Liquid-Crystal Phase Grating," *IEEE Trans. Electron Devices* **26**, 1734–1737 (1979).
17. M. Fritsch, H. Wohler, G. Haas, and D. Mlynski, "Liquid Crystal Phase Modulator for Large Screen Projection," *IEEE Trans. Electron Devices* **36**, 1882–1887 (1989).
18. P. Shannon, W. Gibbons, S. Sun, and B. Swetlin, "Surface-Mediated Alignment of Nematic Liquid Crystals with Polarized Laser Light," *Nature* **351**, 49–50 (1991).
19. P. Bos, J. Chen, and J. Doane, "An Optical Active Defractive Device for a Highly Efficient Light Valve," *Digest of Technical Papers*, Society for Information Display International Symposium, 1995, pp. 601–604.

Received May 10, 1997; accepted for publication March 1, 1998

Kei-Hsiung Yang (K. H. Yang) *IBM Research Division, Thomas J. Watson Research Center, P.O. Box 218, Yorktown Heights, New York 10598 (kyang@us.ibm.com).*
 Dr. Yang received his B.S. in physics from the National Taiwan University, his M.S. from the University of Notre Dame, and his Ph.D. from the University of California at Berkeley in 1974. He joined the IBM Thomas J. Watson Research Center in 1979 as a Research Staff Member; his work in LCD research has included wide-viewing-angle technologies for TFT/LCD, Si-wafer-based LCLVs for reflective projection displays and holographic optical storage, ferroelectric LC devices, TN electro-optics, LC-to-surface anchoring properties, and the transport properties of LC cells. In 1987, he worked at Toshiba Development Laboratories at Shin-Sugita, Japan, for three months as a member of the IBM–Toshiba TFT/LCD joint development team. Prior to joining IBM, Dr. Yang worked at the General Electric R&D Center (1973–1979) in Schenectady, New York; at the Bell Telephone Laboratories (1969) in Murray Hill, New Jersey; and at the Lawrence Livermore Laboratories (1969–1973) in Berkeley, California. Dr. Yang has received a GE Centennial Patent Award, four IBM Invention Achievement Awards, and an IBM Research Division Group Award. He has 16 U.S. patents and nine patents pending, and more than 50 publications in the fields of liquid crystal devices, electrophoretic displays, VUV-fluorescent solids, X-ray imagers for breast cancer diagnosis, and nonlinear optics. Dr. Yang is a member of SID and SPIE.

Minhua Lu ***IBM*** *Research Division, Thomas J. Watson Research Center, P.O. Box 218, Yorktown Heights, New York 10598 (minhua@us.ibm.com).*
 Dr. Lu received a B.S. in physics from the University of Science and Technology of China (1984), an M.S. in materials science from the Chinese Academy of Sciences (1987), an M.S. in physics from Case Western Reserve University (1990), and a Ph.D. in physics from Case Western Reserve University (1992). She joined the IBM Thomas J. Watson Research Center in 1995 as a Research Staff Member and has been working on Si-wafer-based LCLVs for reflective projection displays and holographic optical storage. Prior to joining IBM, she worked for two years as an R&D manager at Kent Display Systems, Kent, Ohio, and for more than half a year as a Postdoctoral Fellow at the Liquid Crystal Institute of Kent State University. She has three U.S. patents and four patents pending, and more than 15 publications in the fields of reflective TN LC devices, fast-switching surface-stabilized cholesteric LCDs including driving, material, and process, polymer-dispersed LC for AMLCDs, and the usage of light scattering to study the polarization and elastic properties of ferroelectric LC and the formation of phospholipid tubules. She is a member of SID and SPIE.